# Does MDCT Really Have a Role in the Evaluation of Neck Masses?

[1]Dr Ravi N, [2]Dr Lakshmeesha M T, [3]Dr Manjappa B H, [3]Dr Naveen K G,
[4]Dr.Ramesh V, [4]Dr.Nagaraj B R
*[1]Associate Professor, [2]Resident, [3]senior resident, [4]Professor and HOD,*
*Department of Radio diagnosis and Imaging, Bangalore medical College and Research institute.*
*Bangalore, Karnataka, India*

***Abstract:***

*100 patients with neck masses were evaluated using multidetector CT. Non-contrast and contrast-enhanced CT examination of all the patients was carried out. The usefulness of CT examination, regarding prediction of the nature of the mass (benign/ malignant), delineation of its extensions, vascular relations, attenuation and enhancement patterns. The findings were correlated with the surgical and histopathological studies. The accuracy of MDCT for predicting the benign or malignant nature of the mass, and its extent was found to be very high. In all cases, the extent of the pathology, the local or contiguous spread and vascular involvement, predicted by MDCT examination corroborated well with the surgical findings. MDCT is the imaging modality of choice for the evaluation of neck masses, because of its increased sensitivity and specificity for the lesion detection and characterization of its relations and extensions.*

**Keywords:** *MDCT, neck masses, benign, malignant, extensions.*

## INTRODUCTION

Neck masses can be grouped into two types: 1). Nodal masses and 2). Non-nodal masses.Both types can appear as benign or malignant lesions[1].Coupled with a detailed physical examination and modern endoscopy, imaging has become indispensable in the characterization and staging of neck pathology. Computed Tomography provides essential information about the deep extension of clinically detected masses and may delineate additional clinically unsuspected lesions[2]. The utilization of Multidetector Computed tomographyhas resulted in improved resolution and significant decrease in scan acquisition time. Other advantages are improved temporal resolution into arterial and venous phases, volume acquisition of data enabling convenient retrospective reconstructions, isotropic viewing and unlimited reformations leading to increased lesion conspicuity[3].

## AIMS AND OBJECTIVES:

- To assess the accuracy of Multidetector Computed Tomography in predicting the location of neck masses
- To differentiate benign and malignant lesions

## MATERIALS AND METHODS:

100 patients with neck mass referred by the clinical departments of Bangalore Medical College and Research Institute (BMC & RI), Bangalore, Karnataka, India to the Department of Radio-diagnosis, BMC & RI were prospectively evaluated using MDCT. Study was conducted between July 2013 to August 2014.Non-contrast and contrast-enhanced CT examination was carried out, using Somatom emotion 6 slice CT scanner (Ms Siemens Ltd.).

## INCLUSION CRITERIA:

- All patients with neck masses referred to Radio-diagnosis department

## EXCLUSION CRITERIA:

- Pregnant mothers
- Impaired RFT
- History of contrast allergy

## PROTOCOL

Initial general neck survey examination was done. Later, a digital lateral scout radiograph starting from the base of the skull to the clavicles was taken for all the cases. Slice thickness was 4mm or 5 mm and later reconstructed at 2.5- 3 mm slices. Plain study was done followed by intravenous contrast study. Protocol was tailored according to the age, weight of the patient and the clinical situation. Dual-phase imaging and angiography sequences, Multiplanar reconstructions with/without volume rendering techniques were done as appropriate. Findings were correlated with the clinical course of disease and/or surgical/histopathological findings**.**

The usefulness of CT examination, regarding the prediction of the nature of mass (benign/ malignant; cystic/solid/ mixed density), its localization (exact organ of origin), its local extent and correlation with final clinical / cytological/ surgical diagnosis, was studied. The accuracy was calculated as the percentage of cases where CT

findings correctly matched with clinical / cytological/ surgical findings.

**RESULTS:**

The present study includes 100 cases of neck masses of various age groups. The age range in the study was from 0 years to 80 years. The largest group of patients (22%) was in 41-50 years age group and second largest group of patients (18%) was in the age range of 31-40 years (TABLE NO 1). 66 cases were males and 34 cases were females with male to female ratio of 1.9:1. The spectrum of the 100 cases in the study is shown in TABLE NO 2.

**Table No. 1: Age Distribution Of Neck Masses**

| AGE GROUP | NUMBER OF CASES | PERCENTAGE (%) |
|---|---|---|
| 0-10 | 14 | 14 |
| 11-20 | 12 | 12 |
| 21-30 | 10 | 10 |
| 31-40 | 18 | 18 |
| 41-50 | 22 | 22 |
| 51-60 | 10 | 10 |
| 61-70 | 08 | 08 |
| 71-80 | 06 | 06 |
| TOTAL | 100 | 100 |

**Table No 2: Spectrum Of Different Neck Masses**

| NECK MASSES | NUMBER OF CASES | PERCENTAGE (%) |
|---|---|---|
| Lymph Nodal mass | 32 | 32 |
| Thyroid lesions | 20 | 20 |
| Vascular Malformations | 12 | 12 |
| Developmental lesions | 8 | 8 |
| Inflammatory lesions | 8 | 8 |
| Salivary gland lesions | 6 | 6 |
| Nerve sheath tumours | 6 | 6 |
| Miscellaneous | 8 | 8 |
| Total | 100 | 100 |

In the present study, lymph nodal masses accounted for 32 cases and rest of 68 cases had non-nodal neck masses. Out of 32 nodal masses, 16 were due to tubercular lymphadenitis (Fig. 2B), 15 were secondaries (Fig. 2A) with primary unknown in 10 cases and one case was a case of Non-hodgkin's Lymphoma (Fig. 1). Malignant nature of the lymph nodes could be predicted accurately on multislice CT in all the patients by radiological findings of rounded contour, absence of hilum, eccentric cortical thickening, ill-defined margins with infiltration of surrounding structures (Fig. 2A) and loss of fat planes or a combination of the above features**.**Multislice CT provided additional information, by localizing the primary in glottis, tongue, gingivo-buccal sulcus and in the pharynx in patients with an unknown primary.

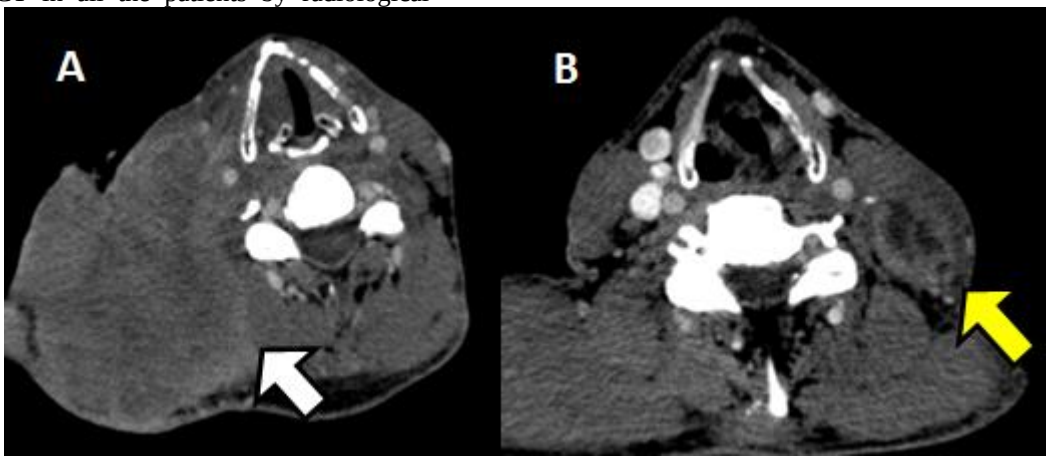


**Fig. 1A and 1B: Metastatic lymph nodal mass and Tubercular lymph node. Axial contrast enhanced CT scan section (1A) showing a large well defined heterogeneously enhancing lesion (white arrow) in the**

**right mid jugular region, with invasion into surrounding structures, consistent with metastatic lymph node secondary to left gingiva-buccal sulcus squamous cell carcinoma. Axial contrast enhanced CT scan section (1B) in a different patient showing a conglomerate mass of multiple hypoattenuation lesions with peripheral enhancement (yellow arrow), in the left posterior triangle consistent with caseous necrotic nodes of Tubercular adenitis.**

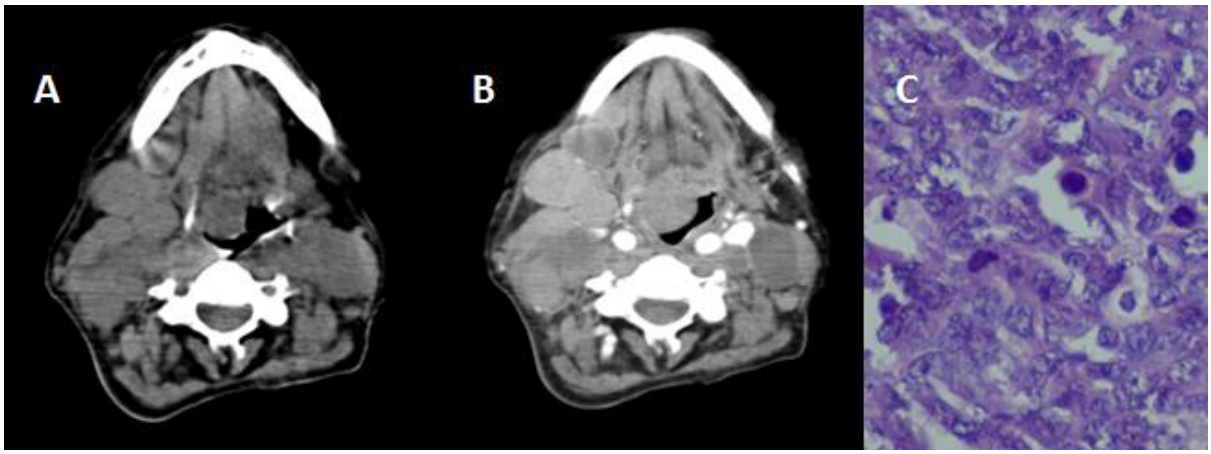


**Fig. 2: Nonhodgkin's Lymphoma. Axial (2A) and contrast enhanced (2B) CT scan sections showing multiple well defined nodular masses soft tissue attenuation masses showing homogenous enhancement in bilateral submandibular and carotid spaces. Histopathology (2C) showing multiple lymphocytes with large nuclei and open chromatin.**

20 patients presented with neck masses of thyroid origin. A female preponderance was noted in patients with thyroid masses. 16 patients hadmultinodular goitre, 3 patients had papillary carcinoma and one patient had an anaplastic thyroid carcinoma. Microcalcification was seen in one case with papillary carcinoma of thyroid. Coarse calcification was seen in both benign as well as malignant pathologies. Patients with multinodular goitre had retrosternal extension better demonstrated with MPR and MIP images achieved using multidetectorCT (Fig. 3B). In the patient with Papillary thyroid carcinoma, multislice CT was able to clearly reveal the presence of vertebral, oesophageal and spinal canal invasion (Fig 4). In one patient, CT showed features of benign thyroid nodule, but on histopathology, it turned out to be papillary carcinoma of thyroid.

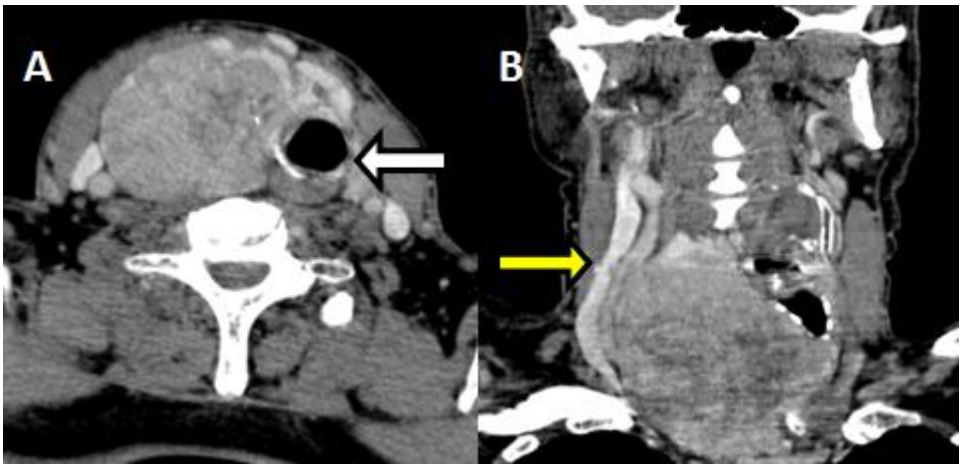


**Fig. 3A and 3B: Multinodular goitre. Axial (3A) and coronal (3B) contrast enhanced CT scan sections showing bulky rightthyroid lobe with multiple heterogenously enhancing nodules. The bulky right lobe is causing mass effect and pushing the trachea towards left (white arrow) and lateral displacement of the**

**right common carotid artery and internal jugular veins (yellow arrows). Inferiorly it is extending into the superior mediastinum.**

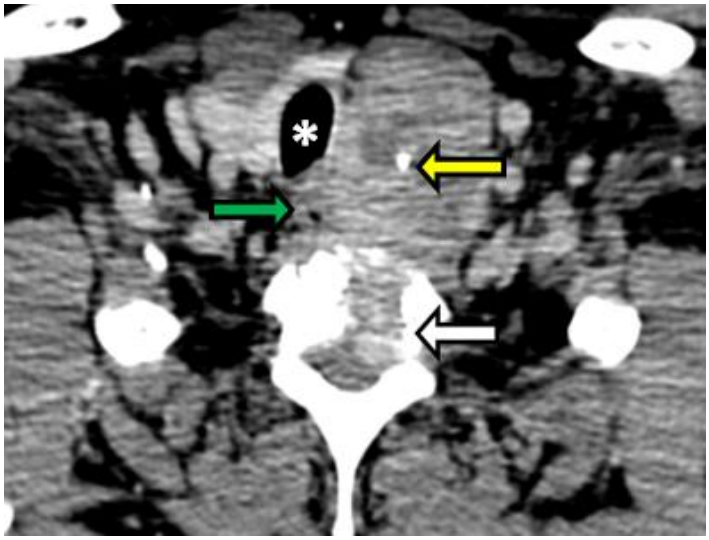

**Fig. 4: Papillary carcinoma of thyroid. Axialcontrast enhanced CT scan sectionshowing bulky left thyroid lobe with a large heterogenously enhancing lesion with central calcific focus and hypodense necrotic areas (yellow arrow). The lesion is causing invasion of the C4 vertebral body (white arrow) with intraspinal extension and compression of the cervical spinal cord. It is also causing tracheal compression (white asterisk) and also loss of fat plane between the cervical oesophagus (green arrow).**

Twelve patients with vascular malformations were evaluated in this study. Four patients had low flow vascular malformations and six patients had high flow vascular malformations and two patients had lymphangioma. Additional unsuspected involvement by multifocal high flow vascular malformation was found in parotid gland and parapharyngeal space in one patient with multidetector CT. Lesions in four patients with low flow vascular malformations showed typical muscle attenuation with mild to moderate, heterogenous, post contrast enhancement with ill-defined margins. In the patient with a high flow vascular malformation a MIP image with Multislice CT very well demonstrated the feeding artery and draining vein (Fig 6B), which were not very well seen on axial images (Fig 5)**.**Lymphangioma showed well defined fluid attenuation lesion with multiple internal septations (Fig. 7).

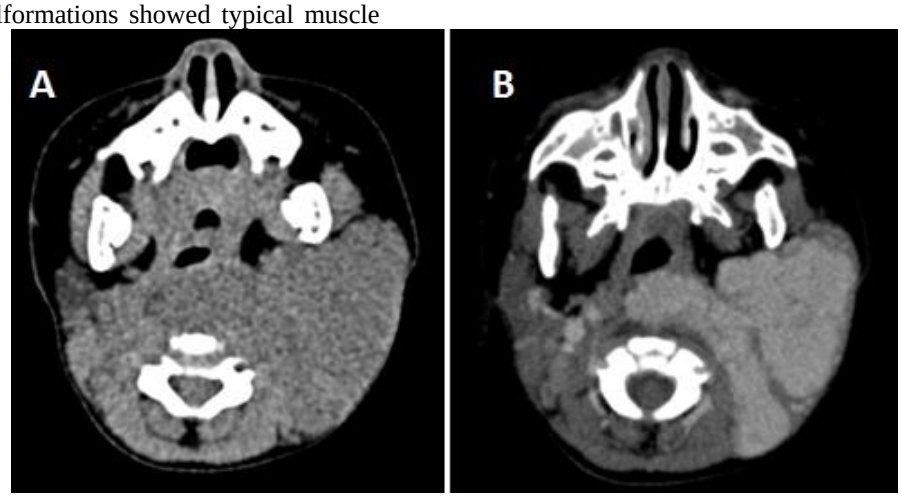


**Fig. 5: Left Parotid gland arteriovenous malformation: axial plain (5A) and contrast enhanced (5B) CT sections showing a large well defined soft tissue attenuation lesion replacing both superficial and deep lobes of left parotid gland and showing intense enhancement. The lesion is extending into left carotid space, left posterior triangle and left retropharyngeal space.**

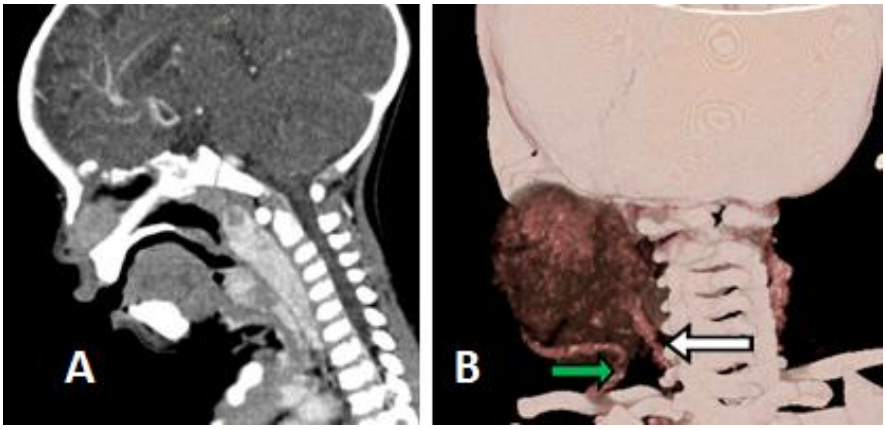


**Fig. 6: Left Parotid gland arteriovenous malformation: sagittal reformatted (6A) contrast CT neck showing a large well defined soft tissue attenuation lesion in the retropharyngeal space, extending into the epiglottis. Volume rendered image (6B), posterior view showing large arteriovenous malformation in left parotid region with feeding arteries arising from the left subclavian artery (green arrow) and left external carotid artery (white arrow).**

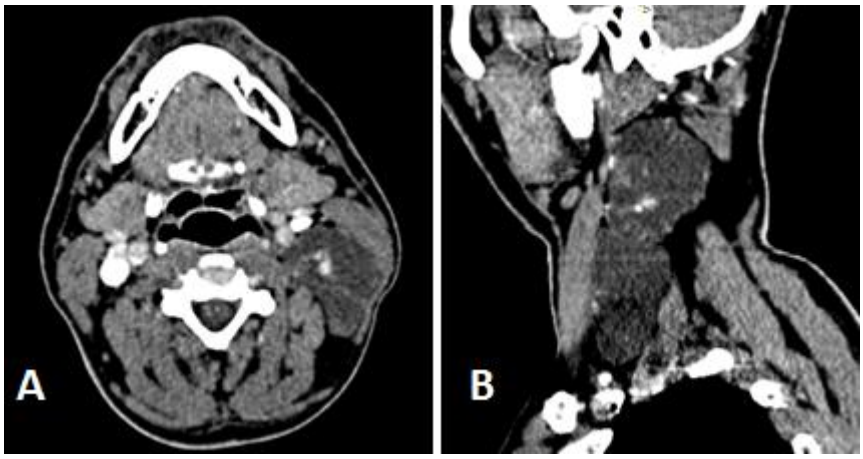


**Fig. 7: Lymphangioma: axial (7A) and sagittal contrast enhanced (7B) CT sections showing a large well defined fluid attenuation lesion in the left posterior triangle. It also shows multiple thin enhancing internal septations.**

Eight patients presented with neck masses of developmental origin. Six cases were branchial cleft cysts and two were thyroglossal duct cysts. Branchial cleft cysts were second branchial cleft cyst (Baileys type II cysts), which showed well defined fluid attenuation lesion anterior to mid third of sternocleidomastoid muscle. Thyroglossal cysts were midline cystic masses in anterior neck, just above hyoid bone, showing rim enhancement.

**Fig. 8: Second Branchial cleft cyst. axial contrast enhanced CT section showing a well defined fluid attenuation lesion with thin rim enhancement, in the left midjugular region, anterior to sternocleidomastoid muscle.**

Eight patients presented with neck masses of inflammatory origin. Six patients had retropharyngeal abscess, one case had cellulitis of neck and one had Ludwig's angina. The patient with retropharyngeal abscess presented with fever and dysphagia. On computed tomography, retropharyngeal abscess showed a fluid attenuation collection with peripheral enhancement, in the retropharyngeal space and causing significant airway compromise (Fig. 9). One patient presented with diffuse swelling of neck and high grade fever following foreign body ingestion, esophageal perforation and mediastinitis. The patient had diffuse neck swelling with significant collection of air in the subcutaneous planes, masticator spaces, carotid spaces, visceral spaces, retropharyngeal and parapharyngeal spaces bilaterally. Another patient had Ludwig's angina, which showed collection of air in the anterior subcutaneous plane and in the bilateral submandibular and submental spaces.

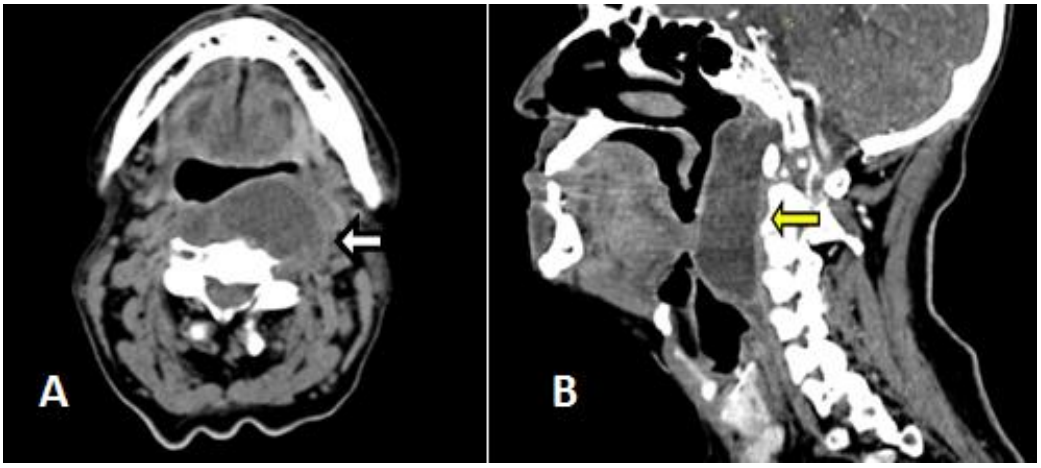


**Fig. 9: Retropharyngeal abscess. Axial (9A) and sagittal (9B) contrast enhanced CT sections showing a well defined peripherally enhancing central fluid attenuation lesion in the retropharyngeal space (white arrow in 9A and yellow arrow in 9B), causing compression of nasopharyngeal and oropharyngeal airway. The collection was extending from the skull base to the C5 vertebral level.**

Six patients had salivary gland lesions, three were benign out of which two were pleomorphic adenomas and one was Warthin's tumour (Fig. 10) and three were malignant parotid tumours.

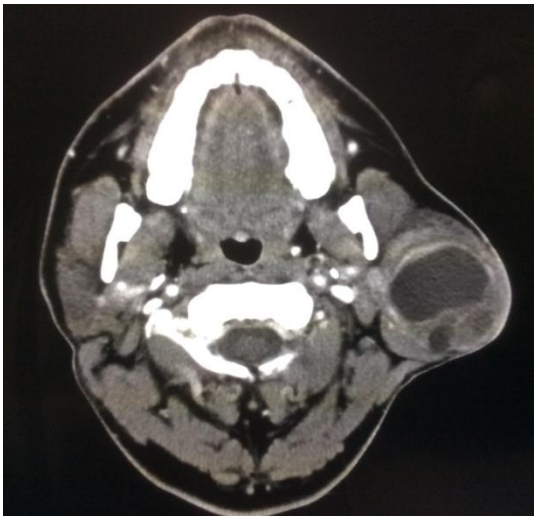

**Fig. 10: Warthin's tumour. Axial contrast enhanced CT section showing a well defined solid cystic lesion in the left parotid gland. The solid part showing enhancement with central nonenhancing cystic area.**

Six patients had nerve sheath tumours (schwannomas). All three were in the carotid space. The lesions showed mild contrast enhancement and were displacing the carotid arteries anteriorly, internal jugular vein posteriorly (Fig. 11). It indicates the lesion was of vagal nerve origin.


**Fig. 11: Left Vagal nerve Schwannoma. Axial (11A) and sagittal (11B) contrast enhanced CT sections showing a well defined heterogeneously enhancing lesion in left carotid space. It is causing anterior displacement of left internal and external carotid arteries (green arrows in Fig 11A and B) and posterior displacement of left internal jugular vein (white arrow in Fig 11A).**

Eight patients showed miscellaneous lesions like lipomas.These were well defined lesions with fat attenuation and multiple internal septations (Fig. 12).Most common site being posterior triangle.

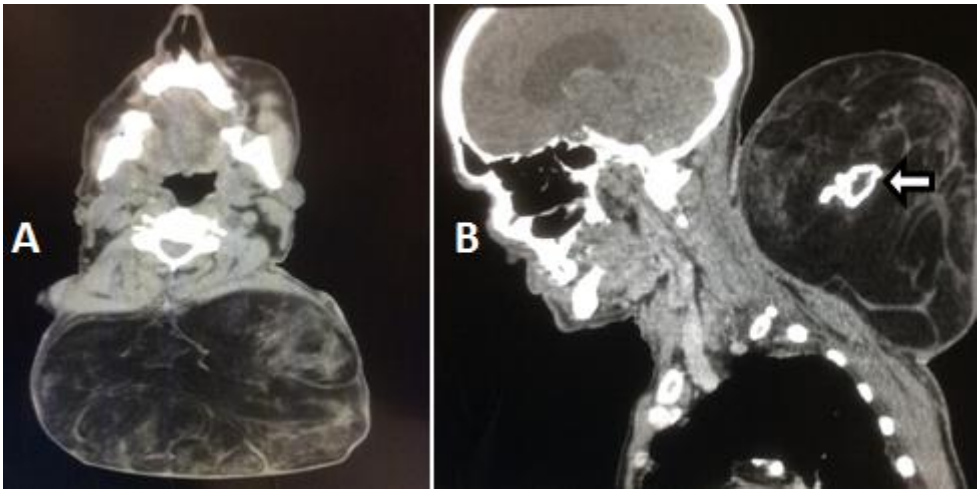


**Fig. 12: Lipoma. Axial (12A) and sagittal (12B) contrast enhanced CT sections showing a large well defined fat attenuation lesion in the posterior neck. The lesion shows multiple thin internal septations and a central dystrophic calcification (white arrow in Fig 12B).**

Computed tomography CT correctly predicted the benign or malignant nature of the lesion in 98/100patients, with an accuracy of 98%. The extent of the lesion predicted by computed tomography correlated well with the surgical findings in all eighty-eight patients in which surgical follow up was available. CT was able to correctly predict the final diagnosis in sixty seven of eighty eight patients with accuracy of 76%. Thus the accuracy of the newer Multislice CT for predicting the benign or malignant nature of the mass and local extent of the mass lesion was found to be very high i.e. 98% and 100% respectively. However CT was 76% accurate in predicting the final pathological diagnosis.

**DISCUSSION:**

CT has proved to be proved to be sensitive and reliable in the evaluation of various disease processes. Coupled with a detailed physical examination and modern endoscopy, imaging has become indispensable in the characterization and staging of neck pathology[2].It is non-invasive, non-operator dependent and permits the accurate measurement of tissue attenuation coefficient. Spiral CT improved the examination quality, reducing the sedation time and requiring lower radiation doses[4].Multi slice spiral CT using multiple detector rows is the latest advancement in CT technology. Use of multiple detector rows allows faster scanning and thinner collimation[5].

MultidetectorCT permits rapid scanning of large volumes of tissue during quiet respiration[6]. Spiral images are less susceptible to patient motion than conventional CT, although image noise is slightly increased. Volumetric helical data permit optimal multiplanar and three-dimensional (3D) reconstructions. Moreover, spectacular CT angiograms can be produced with the data (Fig. 6B )[2].

Excellent 3-Dimensional imaging is possible using volume rendering, maximum Intensity projection and shaded surface display techniques, which helps the operating surgeon to understand the exact extent of the lesion and its relationship to surrounding structures. Thus, the radiologist can point out to the clinician the pathological findings by some essential images without having to demonstrate all axial slices[7].

Intravenous contrast agent is used to study the enhancement characteristics of the lesion. Nonionic contrast is preferred, especially in high-risk, pediatric, or elderly patients in whom the rapid bolus can produce nausea or vomiting[2].

Due to faster speed of scanning, motion related problems have decreased. In addition sedation can be avoided in majority of pediatric patients[8].It remains the best technique for imaging a bony matrix and itis excellent for identifying small soft-tissue calcifications. Nonetheless, CThas its disadvantages. It involves the use of ionizing radiation, which areundesirable in children and pregnant women, it requires an iodine-basedcontrast agent injection, which associated possible risk of allergic reactions,and in certain areas of the neck CT does not provide soft tissue definition
equivalent to that attainable with MR imaging[9].

Commonest neck masses in the present study were lymph nodal masses (32%). Lymph nodes enlarge secondary to either neoplastic or benign processes. Neoplastic lymph nodes can be due to

primary lymphoma or due to secondary to systemic lymphoma, squamous cell carcinomas of aerodigestive tract (gingiva-buccal carcinoma, laryngeal and pharyngeal carcinomas). Benign lymph nodes are due to infections (Tuberculosis, fungal, toxoplasma etc), other systemic diseases like sarcoidosis, Kimura's and castleman's disease. However, because the imaging characteristics in all of these diseases are nonspecific, the diagnosis is based on the combination of history, clinical findings, imaging, and laboratory data. The role of imaging is to locate the node disease and to evaluate any associated findings such as necrosis or abscess formation as well as soft tissue infiltration. The criteria for metastatic disease include the size (short axis diameter should not exceed 11 mm in level II nodes and should not exceed 10 mm at nodes elsewhere in the neck) and shape (loss of normal oval shape), abnormality of the internal architecture (loss of normal central fatty hilum), including nodal necrosis, and extracapsular tumor spread (indicated by indistinct nodal margins, irregular nodal capsular enhancement, or infiltration in the adjacent fat or muscle as seen in Fig. 2A)[1]. CT helps in localising the lesion, delineates the extent and thus helps in staging of the malignancy.

Large homogeneous lymph nodes, sometimes with a thin capsule, are most commonly encountered in lymphoma, sarcoidosis, and infectious mononucleosis. Cross-sectional imaging cannot reliably differentiate Hodgkin's from non-Hodgkin's lymphoma[1].

Tubercular lymphadenitis on CT initially shows homogenous attenuating enlarged nodes, later central hypoattenuation caseous necrosis. There can be matting of nodes and peripheral enhancement. Very rarely, can show calcification in late stages[10].

Three-dimensional reconstructions using shaded surface display (SSD) and maximum intensity projections (MIP) provided additional information by clearly delineating the feeding arteries and draining veins of the parotid arteriovenous malformation(Fig. 6B), which could not be interpreted on axial images[2].

## CONCLUSION

The accuracy of MDCT for predicting the benign or malignant nature of the mass, and its extent was found to be very high. MDCT with its multiplanar imaging capability and newer advances like volume rendering can identify the feeding arteries and draining veins in vascular malformations. It is also helpful in localizing the primary in cases of secondary cervical lymph nodes of unknown primary.CT is a main tool for staging and follow-up of the malignant lesions. MDCT is the imaging modality of choice for the evaluation of neck masses, because of its increased sensitivity and specificity for the lesion detection and characterization of its relations and extensions.

## REFERENCES


[1] Haaga JR et al. CT and MRI of the whole body. 5thed. Mosby Elsevier. 2009;1863-1941.

[2] Lee JKT, Sagel SS, Stanley RJ, Heiken JP, eds. Computed Body Tomography with MRI Correlation, 4th ed. Lippincott Williams and Wilkins, 2006.p.145-214.

[3] Gupta P et al. Role of Multislice C.T. in the evaluation of neck masses. JIMSA Jan-Mar 2013; 26(1): 51-54.

[4] Kalender WA. Principles and applications of spiral CT. Nucl Med Biol 1994;21(5):693-699.

[5] Horton KM, Sheth S, Corl F, Fishman EK.. Multidetector row CT: principles and clinical applications. Critical Reviews in Computed Tomography 2002;43(2):143- 181.

[6] Suojanen JN, Mukherji SK, Dupuy DE, et al. Spiral CT in evaluation of head and neck lesions: work in progress. Radiology 1992;183:281-283.

[7] Greess H, Nomayr A, Tomandl B et al. 2D and 3D visualization of head and neck tumors from spiral CT data. Eur J Radiol. 2000 Mar;33(3):170-7.

[8] Frush DP, Donnelly LF. Helical CT in children: technical considerations and body applications. Radiology 1998;209:37 48.

[9] Som PM. The present controversy over imaging method of choice for evaluating the soft tissues of the neck. American Journal of Neuroradiology 1997;18:1869-72.

[10] Dahnert W. Radiology Review Manual. 7th ed. Lippincott Williams Wilkins 2011;411.